Biochimica et Biophysica Acta, 645 (1981) 243–252
Elsevier/North-Holland Biomedical Press

BBA 79315

A THREE-STATE MODEL FOR INACTIVATION OF SODIUM PERMEABILITY

G. OCHS, B. BROMM and J.R. SCHWARZ

Institute of Physiology, University of Hamburg, Martinistrasse 52, 2000 Hamburg 20 (F.R.G.)

(Received December 12th, 1980)

Key words: Na^+ permeability; Inactivation model; (Myelinated nerve)

The inactivation of Na^+ permeability in single myelinated motor nerve fibres of *Rana esculenta* was investigated under voltage and current clamp conditions at 20°C in Ringer's solution and under blocked K^+ currents. Development of inactivation and its recovery was described by two potential-dependent time constants: The smaller time constant followed the usual bell-shaped function of membrane potential, whereas the larger one was monotone-increasing with more negative potentials. Several three-state models for inactivation were investigated. The experiments could best be approximated by a model with two open and one closed state for inactivation following: open ⇌ closed ⇌ open. Rate constants were determined for all transitions shown from the voltage clamp experiments. The action potentials computed by means of the proposed model were in good agreement with those measured, both in Ringer's solution and under blocked K^+ current conditions.

Introduction

The inactivation of the Na^+ permeability in myelinated nerve is obviously more complex than is implied by a single exponential time course. As already shown by Frankenhaeuser [1] the slope of inactivation depends on the amplitude and duration of the prepulse. Several multi-state models of inactivation have been proposed for the giant axon of the squid [2,3] and the myelinated nerve fibre [4–6]. Since the K^+ current could mask the slow decay of Na^+ inactivation, in all these experiments the K^+ permeability was blocked by tetraethylammonium chloride. Nevertheless, effects of the drug on the Na^+ current have been reported [7]. Furthermore, action potentials under tetraethylammonium chloride show a pronounced plateau phase during repolarisation [8], in disagreement with those predicted from voltage clamp analysis with the K^+ permeability being set zero [9,10].

The present investigation describes experiments on myelinated nerve fibres in which the K^+ current was eliminated in different ways. Development and recovery of Na^+ inactivation was investigated and the contribution of two different processes, a fast and a slow one, was established. Several alternative three-state models for inactivation were discussed and tested for their ability to predict membrane currents and action potentials measured in the same nerve fibre. On this basis we propose a model describing inactivation by transitions between two open and one closed state.

Methods

Experimental setup. The experiments were performed on single myelinated motor nerve fibres of *Rana esculenta* in the arrangement described in detail by Nonner [11]. The node under investigation was continuously superfused with Ringer's solution or test solutions. The neighbouring nodes were cut in isotonic KCl. The temperature of the solutions was adjusted to 20°C. The holding potential was assumed to be −70 mV if $h_\infty = 0.7$ [12]. Potential and current measurements were converted to digital

form (A/D-conversion with 20 μs sampling interval and 8-bit-resolution). Prepulse steps were initiated every 2 s and data were processed by a PDP 11/34 computer. Magnetic tape or disk was used for mass storage.

Solutions. The Ringer's solution contained 110 mM NaCl, 2.5 mM KCl, 1.8 mM $CaCl_2$, and 5 mM Tris-HCl, buffered at pH 7.3. The isotonic KCl solution contained 117 mM KCl. To Ringer's solution either tetrodotoxin (Sankeyo, Tokyo), tetraethylammonium chloride (Merck-Schuchardt, Mannheim) or 4-aminopyridine (Fluka AG, Neu-Ulm) was added.

Data analysis. The analysis of membrane currents was based on the equations of Frankenhaeuser and Huxley [9]; all evaluations were performed without any p current [4,5]. Current calibration followed the procedure of Frankenhaeuser [13]. Leakage (i_l), and capacity current (i_c) were measured by potential steps to $E = -115$ mV, extrapolated to the potentials applied, and subtracted from the measured membrane currents i_m^*, i.e.

$$i_m^* - i_l - i_c = i_m = i_{Na} + i_K \qquad (1)$$

Different impulse programs were chosen to measure recovery and development of inactivation, as given in the insets of the figures. The symbol E will be used in all cases to denote the membrane potential under investigation.

Steady-state values and time constants for the ionic permeabilities were obtained simultaneously by curve fitting from $i_m(t)$. The iterative algorithm employed [14] started from estimated values for the parameters involved, and stopped if no preset improvement in the agreement between the measured and the approximated curve was achieved by the following iteration step. For faster convergence the iterative procedure could be restricted to the non-linear parameters (time constants), with the linear ones (steady-state values) being determined in one last step (for details, see Ref. 15). Thus, usually less than ten iterations were required to reach the convergence criterion. From the extracted data, action potentials could be calculated for the same nerve fibre. A modified Heun-Kutta method was used to solve the differential equation system involved [16].

Results

1. Experimental evidence of two time constants for inactivation

Membrane currents and action potentials in Ringer's solution and solutions containing 10 mM tetraethylammonium chloride were measured. Complete data were obtained from a set of membrane currents at different potentials for the individual nerve fibre, from which action potentials were computed, which could be compared with the measured ones (Fig. 1). In Ringer's solution reasonable agreement was achieved on the basis of the underlying equation system for both membrane currents and action potentials; small deviations may be seen in the decay of currents and potentials. Under tetraethylammonium chloride, however, the deviations increased to an amount which demonstrated systematic inconsistencies in the usual description of Na^+ currents.

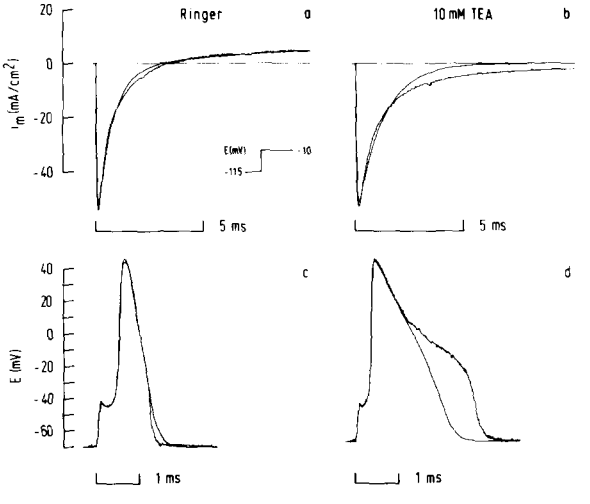

Fig. 1. Membrane currents and action potentials approximated with one time constant for Na^+ inactivation, in Ringer's solution (a, c) and under 10 mM tetraethylammoniumchloride (TEA, b, d). Currents were recorded for a potential step to −10 mV after a 50 ms prepulse of −115 mV (see inset). The smooth curve in a and b represents the best approximation with one time constant for inactivation. Action potentials (c, d) were elicited with 1.0 ms depolarizing current pulses. Smooth curves superimposed on the measured action potentials were calculated by the data extracted from clamp experiments; resting potential: −70 mV in c and −65 mV in d; membrane capacity: 2 μF/cm².

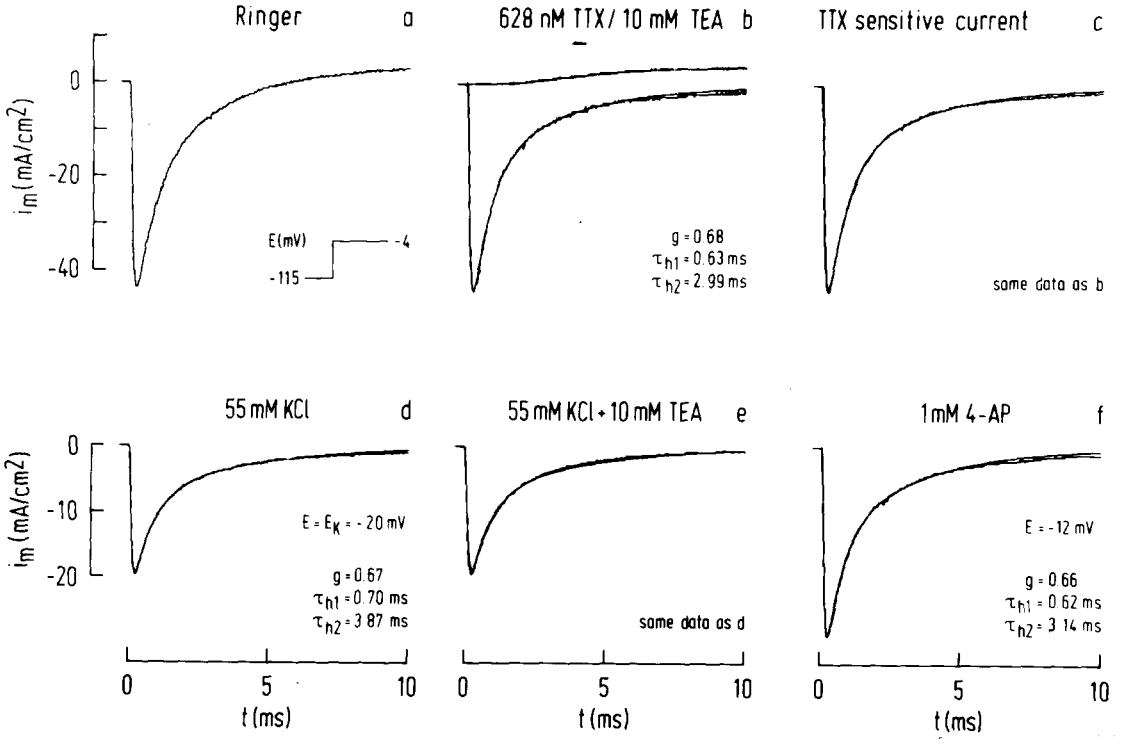

Fig. 2. Membrane currents approximated with two time constants for Na^+ inactivation. Membrane currents were recorded for a potential step of −4 mV after a 50 ms prepulse of −115 mV (see inset), in Ringer's solution (a), in 628 nM tetrodotoxin (TTX, b, upper curve), in 10 mM tetraethylammonium chloride (TEA, b, lower curve). (c) TTX-sensitive current, obtained by subtracting the upper membrane current in (b) from that in (a). (d) Membrane currents in 55 mM KCl during a potential step to $E_K = -20$ mV; (e) the same with 10 mM TEA added to the solution. (f) Membrane current measured in 1 mM 4-aminopyridine (4-AP) associated with a potential step from −115 mV (50 ms) to −12 mV. Best approximations with two time constants for the development of Na^+ inactivation (values given in the insets) were superimposed on the measured currents in (b–f) (see Eqn. 3). Two different motor nerve fibres (a, b, f and d, e), 20°C.

The K^+ current was suppressed in several different ways to exclude the possibility that tetraethylammonium chloride induced a slow decay phase of the Na^+ current. In a first set of experiments the tetrodotoxin-sensitive current was investigated. For this purpose membrane currents were recorded in Ringer's solution and subsequently in 628 nM tetrodotoxin which totally blocked the inward currents (Fig. 2a and b, upper curve). The tetrodotoxin-sensitive current was then obtained by subtracting these two curves (Fig. 2c). These measurements were performed on the same nerve fibre, employing the same potential step of $E = -4$ mV, preceded by a 50 ms prepulse of $E_0 = -115$ mV; the sequence of solution change in this experiment was Ringer's, tetraethylammonium chloride, Ringer's, tetrodotoxin, Ringer's. The tetrodotoxin-sensitive current (Fig. 2c) had the same kinetics as the current under tetraethylammonium chloride (Fig. 2b, lower curve), demonstrating that no chemical influence of the blocking agents occurred (see Eqn. 1).

Another way to exclude any effect of tetraethylammoniumchloride on the Na^+ inactivation was to measure the Na^+ current at the K equilibrium potential E_K. E_K was shifted to $E = -20$ mV by a solution containing 55 mM KCl and, for the sake of isotonicity, 57.5 mM NaCl. At test potentials of −20 mV, therefore, no outward current appeared (Fig. 2d). Under the same conditions 10 mM tetraethylammonium chloride was added to the solutions, which obviously had no effect on the membrane current (Fig. 2e). Further experiments were per-

formed using 4-aminopyridine to block the K^+ permeability (Fig. 2f). As under tetraethylammonium chloride, the K^+ permeability was abolished without any visible effect on the development of Na^+ inactivation.

From the measured Na^+ current the permeability P_{Na} can be calculated [9] by the equation

$$i_{Na} = P_{Na} \cdot \frac{EF^2}{RT} \cdot \frac{[Na]_o - [Na]_i \cdot \exp(EF/RT)}{1 - \exp(EF/RT)} \quad (2)$$

E denotes clamp potential, and $[Na]_o$ resp. $[Na]_i$ the external resp. internal Na^+ concentration at the node; R, T and F have the usual meaning. Following the suggestion of Chiu [4], the current was approximated by a modified inactivation term:

$$P_{Na} = (P_{Na})_{max} \cdot m^b \cdot [g \cdot \exp(-t/\tau_{h1}) + (1-g) \cdot \exp(-t/\tau_{h2})] \quad (3)$$

with $(P_{Na})_{max}$ describing maximum Na^+ permeability, m^b activation, τ_{h1} and τ_{h2} time constants of inactivation, and the coefficients g and $(1-g)$ the relative contributions of both exponential functions. Thus it was assumed that Na^+ activation and inactivation were independent processes. Best results were obtained with an exponent $b = 4$; the other parameters of Eqn. 3 are given in Fig. 2a–f. Fitting the Na^+ currents under different experimental conditions yielded no change in these parameters. The quantitative agreement between the measured and approximated currents obtained by the different methods led to the following conclusions: (1) The experimental procedure used to block the K^+ current had no influence on the remaining membrane current. (2) The development of inactivation could satisfactorily be described by two exponential functions.

Two time constants for the development of inactivation could be distinguished in the potential range investigated: -40 mV $< E <$ +50 mV. In Fig. 3 all data points of one experiment obtained by alternative methods for blocking i_K were plotted versus membrane potential. No dependence of the relative contribution of both inactivation processes from the membrane potential could be observed; thus $g = 0.7 \pm 0.05$ ($n = 6$) in the potential range given above.

Recovery from inactivation was investigated for membrane potentials $E < -40$ mV. A typical experiment is shown in Fig. 4a. The pulse sequence (see inset of Fig. 4b) started with a 500 ms prepulse of $E_0 = -40$ mV, $h_0 = 0$, followed by a conditioning potential of $E = -100$ mV of varied duration t. Recovery from inactivation was measured by a test pulse $E_t = -5$ mV, eliciting the inward currents shown in Fig. 4a. In Fig. 4b the difference between the stationary peak current and each elicited peak current are plotted versus duration of the conditioning pulse t. It must be emphasized that in all motor nerve fibres this duration had to be enlarged up to 100 ms to yield a sufficiently stationary peak value. From the semilogarithmic plot in Fig. 4b two time constants for the recovery from inactivation could always be determined. In all recovery experiments, as in Fig. 4, an initial delay of a few hundred μs was observed, as has been described by Chiu [4].

In a small potential region, -80 mV $< E < -60$ mV, development of inactivation could be analysed by the two pulse procedure as well, starting from

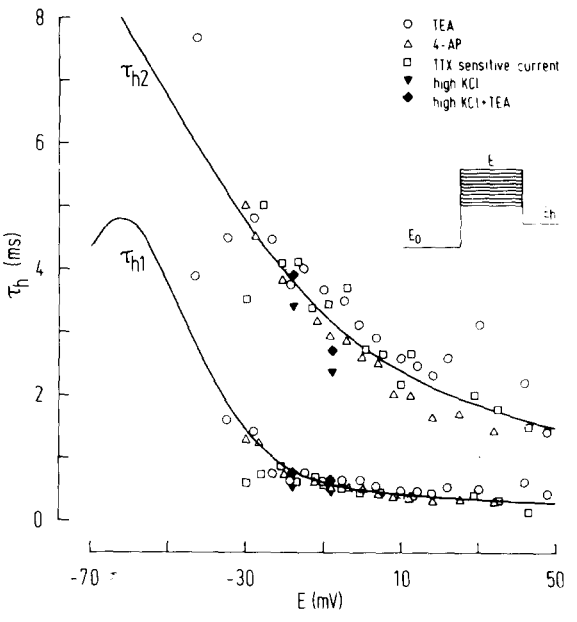

Fig. 3. Development of inactivation; potential dependence of the two time constants τ_{h1} and τ_{h2}. Symbols and pulse program see inset. E_0, 50 ms prepulse of -115 mV; E, depolarizing pulses of several potentials denoted on the abscissa, E_h, holding potential. Smooth curves were determined by the rate constants (Fig. 7) on the basis of the proposed model. All experiments were done on one motor nerve fibre, 20°C.

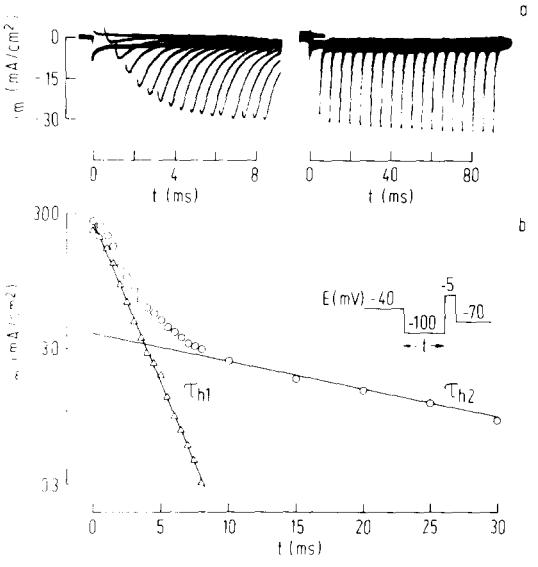

Fig. 4. Recovery from inactivation. Pulse procedure see inset (b). The 500 ms prepulse of $E_0 = -40$ mV fully inactivated the Na^+ permeability ($h_\infty = 0$), it was followed by a conditioning potential to $E = -100$ mV of varied duration t, and recovery from Na^+ inactivation was determined by test pulses of $E_t = -5$ mV. The elicited inward currents were recorded with different beam sweeps on the oscilloscope (a). In (b) the differences Δi_m between actual and stationary ($t = 90$ ms) currents were plotted versus t. The line through the late points (○) yielded τ_{h2}, and differences (△) between this line and the early values yielded τ_{h1}. Motor nerve fibre, 20°C.

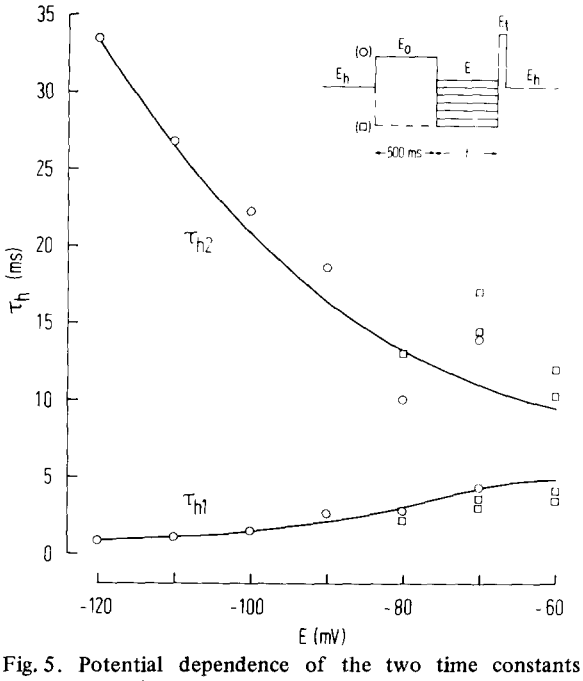

Fig. 5. Potential dependence of the two time constants describing Na^+ inactivation. Pulse program see inset. ○, Recovery from inactivation, $E_0 = -40$ mV ($h_\infty(E_0) = 0$). □, Development of inactivation, $E_0 = -115$ mV ($h_\infty(E_0) = 1$). E_h, holding potential; E, conditioning potential of different duration t followed by the test potential (E_t). Smooth curves were determined by the rate constants (Fig. 7) on the basis of the proposed model. They continue the curves given in Fig. 3 (note different ordinate scales). Motor nerve fibre, 20°C.

$E_0 = -115$ mV, $h_0 = 1$. Again two time constants of inactivation could be determined, the values of which were in agreement with those for recovery for the same potentials. Both time constants were plotted versus E in Fig. 5. The time constant of the fast process was of the same order of magnitude as reported by Frankenhaeuser [1] with the typical bell-shaped potential dependence. In contrast, the time constant of the slow process increased in monotone fashion with more negative membrane potentials; this result was found in all six preparations investigated.

Any major influence of the series resistance on the time course of the Na^+ inactivation is precluded by previous work [4]. In regard to recovery from inactivation, our experiments shown in Figs. 4 and 5 demonstrated that the slow time constant was independent of the actual size of the current. In that potential range, for which both development and recovery could be measured, comparable time constants were found which made any significant contribution of the series resistance improbable.

Whereas no influence of the prepulse on the time constants τ_{h1} and τ_{h2} was found within the pulse program used, the amplitude factor g depended considerably on the conditioning potential. For recovery from inactivation ($E \geq -40$ mV) a value of $g = 0.9 \pm 0.1$ ($n = 5$) was determined, whereas for development ($E = -115$ mV) the fomer value of $g = 0.7 \pm 0.05$ ($n = 5$) was obtained. Because of the smaller contribution of the slow inactivation process during recovery, its measurement was less accurate. In further experiments the potential dependence of the factor g on the amplitude of the conditioning pulse was investigated for -115 mV $\leq E \leq -40$ mV. The pulse was followed by a constant

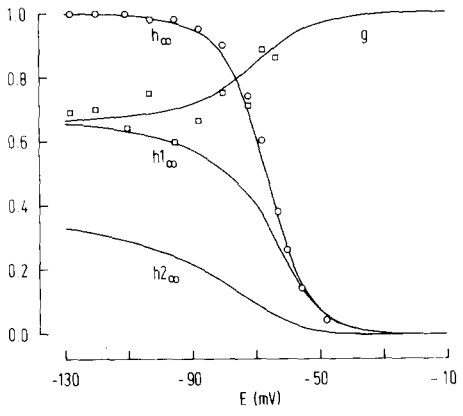

Fig. 6. The fractions of steady state inactivation. h_∞, $h1_\infty$, $h2_\infty$ were calculated using Eqn. 8. Same parameters as in Figs. 3 and 5. The relative contribution $g(E)$ of $h1_\infty = N_1(\infty)$ was evaluated from the decay of Na^+ currents at the same potentials.

potential step to $E_t = +10$ mV, and the decay of the Na^+ currents was approximated by Eqns. 2 and 3, resulting in values for g as function of the potential E. In the same experiments $h_\infty(E)$ was determined from the peak inward currents. As shown in Fig. 6, the amplitude factor g of the fast process increased from about 0.7 at a conditioning potential $E = -115$ mV to 0.98 at $E = -40$ mV. The continuous lines in the figure were calculated on the basis of the following data analysis (model III, Eqns. 7 and 8). In agreement with the findings of Chiu [4], the measured as well as the computed $h_\infty(E)$ curve was asymmetrical.

2. A three-state model describing inactivation of Na^+ permeability

In recent years several types of three-state-models for inactivation have been discussed [4,5,17]. From a general point of view four different three-state-models are possible:

	$N_1 \rightleftharpoons N_2 \rightleftharpoons N_3$		
I	O	C_1	C_2
II	C	O_1	O_2
III	O_1	C	O_2
IV	C_1	O	C_2

(4)

where N_i, $i = 1, 2, 3$ denote the partial occupancy of the states of the inactivation system, O that of the open, C that of the closed states. The scheme (4) distinguishes two groups of reaction systems: In I and II the transitions occur from left to right or from right to left, in III and IV from both sides to the middle state or vice versa.

The time dependence of all three-state-systems (I–IV) can be described by the following linear differential equation system (cf. Refs. 4 and 5):

$$\begin{aligned}\dot{N}_1 &= -a_{12} \cdot N_1 + a_{21} \cdot N_2 \\ \dot{N}_2 &= a_{12} \cdot N_1 - (a_{23} + a_{21}) \cdot N_2 + a_{32} \cdot N_3 \\ \dot{N}_3 &= a_{23} \cdot N_2 - a_{32} \cdot N_3 \\ \text{with } N_1 &+ N_2 + N_3 = 1,\end{aligned} \tag{5}$$

where a_{ij}, $i, j = 1, 2, 3$ denote the rate constants. From these, two time constants of inactivation can be determined by inverted eigenvalues according to

$$\tau_{h1,2} = 2/(C_2 \pm \sqrt{C_2^2 - 4C_1}) \tag{6}$$

with

$$C_2 = a_{12} + a_{21} + a_{23} + a_{32}$$

$$C_1 = a_{21}a_{32} + a_{23}a_{12} + a_{32}a_{12}$$

For any constant potential the time dependent solution of Eqn. 5 can be written as

$$N_i(t) = N_i(\infty) + A_i \cdot \exp(-t/\tau_{h1}) + B_i \cdot \exp(-t/\tau_{h2})$$
$$i = 1, 2, 3 \tag{7}$$

with

$$A_i = [\dot{N}_i(0) - (N_i(\infty) - N_i(0))/\tau_{h2}]\tau_{h1} \times \tau_{h2}/(\tau_{h1} - \tau_{h2})$$

$$B_i = N_i(0) - N_i(\infty) - A_i$$

From $\dot{N}_i(\infty) = 0$ follows with Eq. 5:

$$N_1(\infty) = a_{21} \cdot a_{32}/C_1, \quad N_2(\infty) = a_{32} \cdot a_{12}/C_1,$$
$$N_3(\infty) = a_{23} \cdot a_{12}/C_1 \tag{8}$$

All these solutions are independent of the actual meaning of N_i, i.e. whether N_i denotes open or closed conductance states.

The values $N_i(0)$ and $N_i(\infty)$ are determined by the experimental conditions: At extreme membrane potentials, development of inactivation describes the

transition from $h_0 = 1$ to $h_\infty = 0$, recovery the transition from $h_0 = 0$ to $h_\infty = 1$. By the different experimental conditions both reaction types, either I/II or III/IV, can be tested. Of course, the amplitude factor (cf. Eqn. 3) changes sign, if recovery experiments are described. In any case h denotes the number of open states, for example recovery from inactivation, in model III:

$$h = N_1 + N_3\,, \quad -g = A_1 + A_3\,, \quad -(1-g) = B_1 + B_3$$

The four rate constants a_{ij} of Eqn. 5 can be obtained from the measured values of τ_{h1}, τ_{h2}, h_∞ and amplitude factor g. For this purpose we make the usual assumption that two of the rate constants are monotone-increasing functions of membrane potential, while the other two decrease with membrane potential.

Table I demonstrates that in the models I and II for extreme conditions ($h_0 = 0$ and $h_0 = 1$) the time constants are the reciprocal values of the rate constants, whereas in models III and IV there appear combinations of the rate constants a_{ij}. Under the asymptotic conditions for the a_{ij} shown in the first column, only models III and IV tend to increasing τ_{h2} at extreme membrane potentials. By this reason model III comes out to be the only one to account for the increasing slope of τ_{h2} in recovery from inactivation, as observed in all experiments (cf. Figs. 4 and 5); for model IV the increasing values would have been observed during development of inactivation.

Furthermore, the measured amplitude factor g has to be taken into account. The sequential scheme I predicts the slow process to be predominant during recovery, because $N_2(0) = 0$, $g = \tau_{h1}/(\tau_{h1} - \tau_{h2}) \approx 0$, $|1 - g| \approx 1$, in disagreement with the experiments. In model III the fast process is predicted to be most important ($g \approx 1$), which was found in all measurements. In addition, if development is regarded, model IV will yield a factor of $g \approx 1$, i.e., only one time constant would have been observed, in contrast to the experimentally determined value of $g = 0.7$.

Therefore, only the model III seems to be suitable to account for the experimental findings described in this paper. The usefulness of model III became still more evident when the rate constants were exactly determined for all membrane potentials investigated. They are given for model III in Fig. 7 for the experiments presented in Figs. 3 and 5.

Further evidence for the validity of model III was obtained from the prediction of action potentials. For this purpose Eqn. 5 was introduced in the numerical integration procedure, which is described elsewhere [16]. Fig. 8a shows the action potential measured in Ringer's solution at 20°C. In Fig. 8b the computations were based on model I, which was proposed by Chiu [4], and in Fig. 8c the three-

TABLE I

ASYMPTOTIC BEHAVIOUR OF TIME CONSTANTS AND AMPLITUDE FACTORS FOR Na^+ INACTIVATION

Columns indicate: 1, asymptotic conditions; 2 and 6, model describing development or recovery of inactivation; 3 and 5, time constants for the fast process and amplitude factor; 4, time constants for the slow process.

1 preset	2 development	3 τ_{h1}	4 τ_{h2}	5 g	6 recovery
$a_{12} >> a_{21}$ $a_{23} >> a_{32}$	I	$\frac{1}{a_{12}}$	$\frac{1}{a_{23}}$	1	II
$a_{21} >> a_{12}$ $a_{32} >> a_{23}$	II	$\frac{1}{a_{21}}$	$\frac{1}{a_{32}}$	$\frac{-\tau_{h1} + \tau_{h2}N_2(0)}{\tau_{h2} - \tau_{h1}}$	I
$a_{12} >> a_{21}$ $a_{32} >> a_{23}$	III	$\frac{1}{a_{12}}$	$\frac{1}{a_{32}}$	$N_1(0)$	IV
$a_{21} >> a_{12}$ $a_{23} >> a_{32}$	IV	$\frac{1}{a_{21} + a_{23}}$	$\frac{a_{21} + a_{23}}{a_{21} + a_{32} + a_{23} \cdot a_{12}}$	1	III

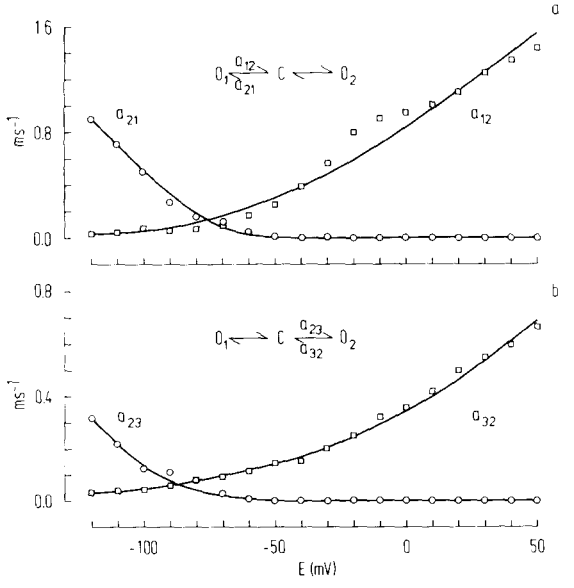

Fig. 7. Rate constants evaluated from the measured data τ_{h1}, τ_{h2}, h_∞, and g, on the basis of model III. The curves were fitted from the experiments in Figs. 3–5, according to the arbitary function of the form [9]

$$a_{ij} = A(B - E)/(1 - \exp(-(B - E)/C))$$

These curves were used to calculate the potential dependence of τ_{h1}, τ_{h2}, and h_∞ in Figs. 3, 5, and 6.

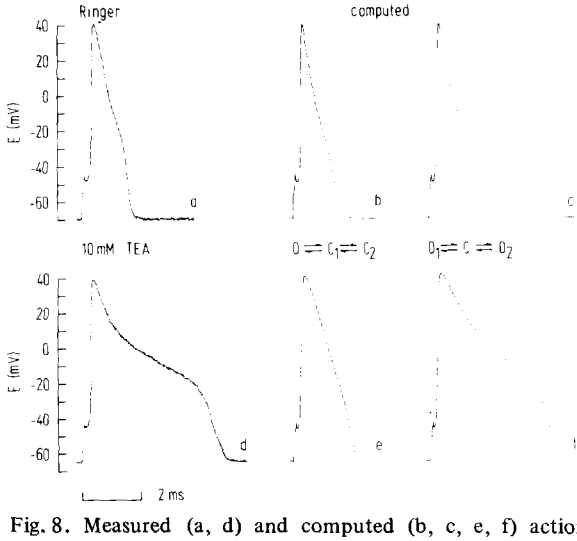

Fig. 8. Measured (a, d) and computed (b, c, e, f) action potentials in Ringer's solution and under 10 mM TEA. The calculation of the action potentials based on different models (b, e: model I; c, f: model III), assuming a resting potential of −70 mV (b, c) or −65 mV (e, f) and a membrane capacity of 2 $\mu F/cm^2$. Motor nerve fibre, 20°C.

state-model III was used for computation. In case of Ringer's solution, when the K^+ current masked the effects of Na^+ inactivation, no significant differences between the models were encountered. In both cases a typical two-phase decay in the action potential appeared, in agreement with the experimental findings on motor nerve fibres. Blocking the K^+ permeability enlarged the plateau phase in the repolarisation of the spike (Fig. 8d, see also Fig. 1c). Obviously model I was unable to predict action potentials correctly; no marked prolongation in its decay could be obtained. It was only the three-state-model III which corresponded to the measured behaviour, qualitatively and quantitatively (Fig. 8f). The data for all computations were evaluated from voltage clamp experiments on the same nerve fibre.

Discussion

The inactivation of the Na permeability proceeded with two time constants throughout the potential range investigated. The potential dependence of the time constant $\tau_{h1}(E)$ of the fast process followed the wellknown bell-shaped curve [18]. In contrast, the slow process exhibited monotone-increasing values of $\tau_{h2}(E)$ with increasing negative membrane potentials. The relative contribution of the two exponential functions depended on the pulse procedure: During development of inactivation the contribution of the slow process was about 30%, whereas during recovery its amount continuously decreased with more negative prepulse potentials. Several three state models were examined, of these only the model $O_1 \rightleftharpoons C \rightleftharpoons O_2$ (O for open, C for closed states) was able to describe Na^+ inactivation in agreement with all experimental findings.

In 1977 Chiu [4] described, for the first time, experiments on the nodal membrane which demonstrated two different processes for the development of inactivation of the Na^+ channel in a potential range $E > -40$ mV. These findings were meanwhile proven by several authors [5,6,19]. With two pulse experiments, two time constants for the development of inactivation could further be established even near resting potential [5]. Nevertheless, all these authors observed only one exponential function responsible for the recovery process, i.e. for mem-

brane potentials $E < -70$ mV. Particularly the detection of two time constants in this potential range, as well as the remarkable differences in their potential dependence, gave evidence in support of the model selected in this paper. In order to detect the slow process during recovery it was necessary to prolong sufficiently the duration of the conditioning pulse potential to at least 100 ms. This was a larger observation time than is usually chosen in such experiments. Furthermore it should be noted that our experiments were performed solely on motor nerve fibres. Sensory fibres may have a different ratio of amplitude factors for the fast and slow inactivation process [20].

It could be assumed that two independent pore populations, each following the Hodgkin-Huxley formalism [18], were responsible for the two exponential functions of inactivation. This possibility, however, was ruled out by the experimental finding that the time constant τ_{h2} for the slow process did not follow the bell-shaped potential dependence, but increased with more negative membrane potentials, while the contribution of the slow process approached zero. The potential dependence found for τ_{h2} implied that the backward rate constant of inactivation decreased, in disagreement with the postulations of Hodgkin and Huxley [18]. Further objections against this assumption could be demonstrated by nonsuccess in computing action potentials with the clamp data under blocked K^+ currents.

Chiu [4] interpreted his results by a three-state model of the form $O \rightleftharpoons C_1 \rightleftharpoons C_2$, which is identical with model I in our paper. In fact, this model is also suitable to describe the membrane currents during development of inactivation ($E > -40$ mV). In this potential range his model, as well as model III, led to similar accuracy in curve fitting. The formal extension of model I to potentials $E < -70$ mV, however, resulted in time constants , which both decreased with more negative membrane potentials, whereby the slow process became dominating. These results were in contradiction to the experimental findings during recovery from inactivation. In contrast, model III predicted precisely that potential dependence of both time constants, as well as that of the relative contributions of both processes to inactivation as was found in all measured Na currents.

A formally equivalent model (III) of the form $O_1 \rightleftharpoons C \rightleftharpoons O_2$ was used by Chandler and Meves [17] to describe the incomplete inactivation in squid axons perfused with NaF. The existence of a second conducting state became apparent with increasing membrane potentials. This indicates that the equilibrium in the reaction scheme $N_1 \rightleftharpoons N_2 \rightleftharpoons N_3$ was at the right at zero membrane potential ($E = 0$), whereas in our experiments the state occupied at this potential was N_2. The Chandler-Meves secondary conducting state, found under NaF, should therefore not be confused with the model proposed here.

In agreement with other investigators [4,5] we found an initial delay during recovery from inactivation. The existence of a delay of this kind, however, can be derived theoretically under the assumption of two time constants as a common feature of all kinetic schemes having three conductance states. Therefore, this observation is no criterion for the selection of one model.

Additional support for the selection of the proposed model was obtained through comparison of measured action potentials with those predicted by different second order reaction schemes. Models I, II and IV did not explain sufficiently the plateau phase during repolarisation of the action potentials observed when experiments were performed under blocked K^+ current conditions. Although some values, such as membrane capacitance or resting potential, could not precisely be determined in the voltage clamp experiments, it should be mentioned that all these parameters remained equal for all the computations. Thus differences in these values should not affect the comparison; differences in the individual spikes must be due to the different models.

Recent investigations of current fluctuations in the nodal membrane [21] gave further evidence of a second open state in the inactivation system. They showed that the transition from the open to the closed state proceeded more slowly in the late phase of the depolarisation than in the early phase at the same potential. This finding is inconsistent with models which have only one kinetic state corresponding to the open channel.

In conclusion, the model proposed seemed to be the most probable among the alternatives discussed. Nevertheless the validity of other multi-state models could not be excluded on the basis of the data

presented; however, hypotheses which were in contradiction to the experimental results could be rejected.

Acknowledgement

We gratefully acknowledge Professor B. Neumcke for reading a first draft of the manuscript. We also wish to thank Dip. math. R. Spielmann for help with the mathematical treatment of the models describing inactivation. This study was supported by the Deutsche Forschungsgemeinschaft, Br. 310/14.

References

1 Frankenhaeuser, B. (1963) J. Physiol. 169, 445–451
2 Bezanilla, F. and Armstrong, C.M. (1977) J. Gen. Physiol. 70, 549–566
3 Armstrong, C.M. and Bezanilla, F. (1977) J. Gen. Physiol. 70, 567–590
4 Chiu, S.Y. (1977) J. Physiol. 273, 573–593
5 Nonner, W. (1980) J. Physiol. 299, 573–603
6 Neumcke, B., Schwarz, W. and Stämpfli, R. (1980) Biochim. Biophys. Acta 600, 456–466
7 Koppenhöfer, E. (1967) Pflügers Arch. 293, 34–55
8 Schmidt, H. and Stämpfli, R. (1966) Pflügers Arch. 287, 311–325
9 Frankenhaeuser, B. and Huxley, A.F. (1964) J. Physiol. 171, 302–315
10 Bromm, B., Ochs, G. and Schwarz, J.R. (1978) J. Physiol. 284, 150P–151P
11 Nonner, W. (1969) Pflügers Arch. 309, 176–192
12 Stämpfli, R. and Hille, B. (1976) Handbook of Frog Neurobiology, eds. (Llinas, R. and Precht, W.), pp. 3–32, Springer, Heidelberg and New York
13 Frankenhaeuser, B. (1962) J. Physiol. 160, 40–45
14 Marquardt, D.W. (1963) J. Soc. Ind. Appl. Math. 11, 431–441
15 Bromm, B., Schwarz, J.R. and Ochs, G. (1981) J. Theoret. Neurobiol., in the press
16 Bromm, B. and Frankenhaeuser, B. (1968) Pflügers Arch. 299, 357–363
17 Chandler, W.K. and Meves, H. (1970) J. Physiol. 211, 679–705
18 Hodgkin, A.L. and Huxley, A.F. (1952) J. Physiol. 117, 500–544
19 Kniffki, K.-D., Siemen, D. and Vogel, W. (1981) J. Physiol. 313, 37–48
20 Schwarz, J.R., Weytjens, J., Ochs, G. and Bromm, B. (1980) Neurosci. Lett. Suppl. 5, 435
21 Sigworth, F.J. (1981) Biophys. J. 34, 111–133